CHEMISTRY

The elusive cyclotriphosphazene molecule and its Dewar benzene–type valence isomer (P_3N_3)

Cheng Zhu[1,2]*, André K. Eckhardt[3,*†], Alexandre Bergantini[1,2‡], Santosh K. Singh[1,2], Peter R. Schreiner[3§], Ralf I. Kaiser[1,2§]

Although the chemistry of phosphorus and nitrogen has fascinated chemists for more than 350 years, the Hückel aromatic cyclotriphosphazene (P_3N_3, 2) molecule—a key molecular building block in phosphorus chemistry—has remained elusive. Here, we report a facile, versatile pathway producing cyclotriphosphazene and its Dewar benzene–type isomer (P_3N_3, 5) in ammonia-phosphine ices at 5 K exposed to ionizing radiation. Both isomers were detected in the gas phase upon sublimation via photoionization reflectron time-of-flight mass spectrometry and discriminated via isomer-selective photochemistry. Our findings provide a fundamental framework to explore the preparation of inorganic, isovalent species of benzene (C_6H_6) by formally replacing the C—H moieties alternatingly through phosphorus and nitrogen atoms, thus advancing our perception of the chemical bonding of phosphorus systems.

INTRODUCTION

Ever since the pioneering discovery of the p-block element phosphorus by the alchemist Hennig Brand 350 years ago (*1*), phosphorus allotropes such as white, red, and black phosphorus along with phosphorous heterocycles such as the diphosphatriazolate anion ($P_2N_3^-$, **1**) (*2*) and cyclotriphosphazene (P_3N_3, **2**; Fig. 1) (*3*, *4*) have captivated the interest of the theoretical, physical (in)organic, preparative, and organometallic chemistry communities (*1*) from the fundamental viewpoints of electronic structure (*5*, *6*) and chemical bonding (*7*, *8*), with both heterocycles representing benchmarks of a class of exotic inorganic $(4n + 2)\pi$ aromatic molecules. Whereas **1** is isovalent to the cyclopentadienyl anion (**3**), **2** can be linked to the prototype 6π-Hückel aromatic (*9*) benzene molecule (C_6H_6, **4**) by formally replacing the C—H moieties alternatingly by isovalent phosphorus (P) and nitrogen (N) atoms. This leads to a planar, D_{3h} symmetric **2** molecule compared to a D_{6h} point group of benzene (C_6H_6, **4**), with both molecules holding $^1A_1$ electronic ground states (*5*, *10*).

Cyclotriphosphazene (**2**) has received particular attention as the prototype of a hydrogen-deficient, inorganic Hückel aromatic system. The distinct Pauling electronegativities of nitrogen (3.0) and phosphorus (2.2) result in a less efficient delocalization of the π electrons and hence diminished aromaticity compared to benzene (C_6H_6, **4**). This is supported by nucleus-independent chemical shifts (NICSs) of −3.9 parts per million (ppm) (h = 1.0 Å) and −10.2 ppm (h = 1.0 Å) for **2** and benzene (C_6H_6, **4**), respectively (*6*, *7*), along with the charge population analysis suggesting positive and negative partial charges on the phosphorus and nitrogen atoms, respectively (*5*). Similarities in the isovalent **4**-**2** system are evident from the molecular structures of the thermodynamically less stable bicycle [2.2.0]hexa-2,5-diene ("Dewar benzene") (**6**; +354 kJ mol^{-1}) (*11*) and 1,3,5-triphosha-2,4,6-triazabicyclo [2.2.0]hexa-2,5-diene (**5**; +155 kJ mol^{-1}) valence isomers (Fig. 1), with the latter only predicted theoretically to exist (*8*). Although **2** core-based dendrimers (*12*) and bulky moieties such as diphenyl (*13*) are stable at room temperature, the parent compound **2** has not been undeniably prepared. Matrix isolation studies by Atkins and Timms (*3*) at 10 K tentatively assigned a cyclic [phosphorusmononitride (PN)]$_3$ isomer via infrared spectroscopy through absorptions at 1137 and 718 cm^{-1}, with Schnöckel and co-workers (*4*) validating the aforementioned analysis. Therefore, despite tentative evidence for the existence of **2**, the preparation and isolation of **2** in the gas phase have eluded synthetic chemists. Considering the difficulties in preparation, short lifetimes above 50 K, and the tendency for polymerization, free cyclotriphosphazenes are one of the least explored classes of inorganic molecules.

RESULTS

Here, we report on the first preparation of **2** along with its Dewar benzene–type valence isomer **5** by exposing low-temperature (5 K) ammonia (NH_3) + phosphine (PH_3) ices to ionizing radiation in the form of energetic electrons. By combining our experiments with electronic structure computations on the P_3N_3 potential energy surface, both isomers were unambiguously identified via photoionization reflectron time-of-flight mass spectrometry (PI-ReTOF-MS) during the temperature-programmed desorption (TPD) phase of the irradiated ices based on their adiabatic ionization energies (IEs), mass shifts upon ^{15}N substitution, and their distinct photoreactions at λ = 452 nm and λ = 388 nm, respectively. By identifying **2** and **5**, this study provides a deeper understanding of the molecular structures and (photo)reactivities of previously obscure heteroaromatic, inorganic molecules (P_3N_3) along with their valence isomers, thus advancing our perception how we think about chemical bonding of phosphorus in aromatic systems.

Fourier transform infrared spectroscopy

The ammonia-phosphine ices were monitored during the irradiation at 5 K via Fourier transform infrared (FTIR), which excels in identifying

[1]Department of Chemistry, University of Hawaii at Manoa, 2545 McCarthy Mall, Honolulu, HI 96822, USA. [2]W. M. Keck Laboratory in Astrochemistry, University of Hawaii at Manoa, 2545 McCarthy Mall, Honolulu, HI 96822, USA. [3]Institute of Organic Chemistry, Justus Liebig University, Heinrich-Buff-Ring 17, 35392 Giessen, Germany and Center for Materials Research (LaMa), Justus Liebig University, Heinrich-Buff-Ring 16, 35392 Giessen, Germany.
*These authors contributed equally to this work.
†Present address: Department of Chemistry, Massachusetts Institute of Technology, Cambridge, MA 02139, USA.
‡Present address: Centro Federal de Educacao Tecnologica Celso Suckow da Fonseca - CEFET/RJ, Av. Maracana 229, 20271-110, Rio de Janeiro, Brazil.
§Corresponding author. Email: ralfk@hawaii.edu (R.I.K.); prs@uni-giessen.de (P.R.S.)

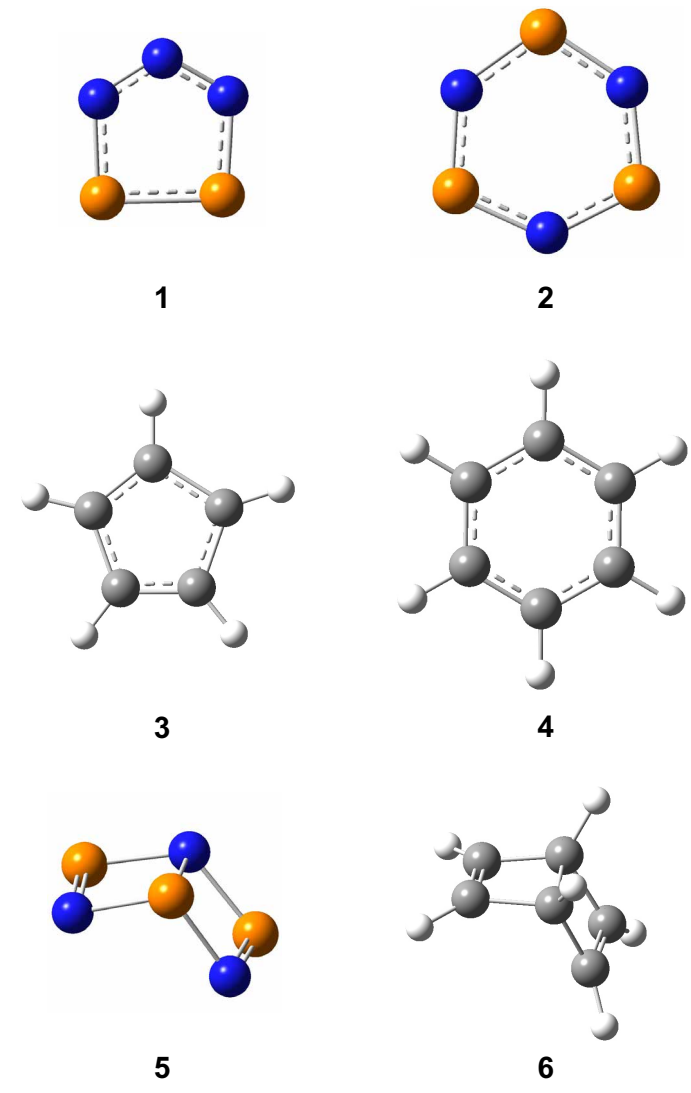

Fig. 1. Molecular structures of (4*n* + 2) (*n* = 1) π-aromatic heterocycles: The diphosphatriazolate anion ($P_2N_3^-$, 1) and cyclotriphosphazene (P_3N_3, 2) along with their isovalent cyclopentadienyl ($C_5H_5^-$, 3) and benzene (C_6H_6, 4) counterparts. The Dewar benzene–type molecular structures of the valence isomers 1,3,5-triphosha-2,4,6-triazabicyclo[2.2.0]hexa-2,5-diene (**5**) and bicycle [2.2.0]hexa-2,5-diene (**6**) are also shown. The atoms are color coded in black (carbon), white (hydrogen), blue (nitrogen), and orange (phosphorous).

small, individual molecules and functional groups of complex molecules (fig. S1 and table S2). Radiation exposure produced seven new absorptions: 3039 cm^{-1} (ν_{N-H}), 2782 cm^{-1} [N═NH_2 (ν_5)], 2235 cm^{-1} (ν_{P-H}) (*14*), 2085 cm^{-1} ($\nu_{N\equiv N}$), 1506 cm^{-1} [•NH_2 (ν_2)], 1153 cm^{-1} [$\nu_{(P=N)}$], and 720 cm^{-1} (—NH_2 wagging) (*15*–*18*). These assignments were firmed up by performing experiments with ^{15}N-labeled ice precursors (table S2), which induced red shifts for the nitrogen-bearing functional groups. The P═N stretching at 1153 cm^{-1} could be associated to multiple P_3N_3 isomers carrying the PN moiety (table S3). However, infrared spectroscopy alone cannot identify individual P_3N_3 isomers as their absorptions fall in a similar range. Hence, an alternative analytical technique is necessary to probe discrete isomers selectively.

Photoionization reflectron time-of-flight mass spectrometry

Therefore, we exploited PI-ReTOF-MS during the TPD phase of the irradiated ices to 300 K (*19*). This method represents a unique approach to detecting gas-phase molecules isomer-selectively via soft photoionization based on their distinct IEs by systematically tuning the photon energies above and below the IE of the isomer(s) to be identified. This results in the identification of the parent ions at well-defined mass/charge ratio (*m/z*). Considering the computed IEs of the P_3N_3 isomers (Fig. 2 and table S3), a photoionization energy (PE) of 10.49 eV (λ = 118.22 nm) was first chosen to ionize all isomers except **9** (IE = 11.10 eV) and **10** (IE = 10.54 eV); thereafter, we selected a photon energy of 9.10 eV (λ = 136.25 nm), which can only ionize isomers having IEs less than 9.10 eV (**7**, **8**, **11**, **12**, **13**, and **14**) but not the target isomers **2** (IE = 9.28 eV) and **5** (IE = 9.32 eV) (Fig. 3). By comparing the TPD profiles at *m/z* = 135 ($P_3N_3^+$) at 10.49 and 9.10 eV, isomers **2** and/or **5** could be identified. The mass spectra of the subliming molecules are compiled in detail in Fig. 3 as a function of temperature. Focusing on the P_3N_3 isomers, we extracted the TPD profiles of ions at *m/z* = 135 ($P_3N_3^+$) (Fig. 4). At 10.49 eV, three sublimation peaks centered at 215, 237, and 256 K are observed (Fig. 4A). Upon tuning to 9.10 eV, below the IEs of **2** and **5**, the first sublimation event is still present, while the latter two peaks vanish (Fig. 4B). These findings suggest that the first sublimation events can be linked to **7**, **8**, **11**, **12**, **13**, and/or **14**, whereas the two later ones correlate with **2** and/or **5**. In separate experiments exploiting ^{15}N-substituted ammonia ($^{15}NH_3$- PH_3 system) at 10.49 eV, signal shifted from *m/z* = 135 by 3 atomic mass unit to *m/z* = 138 ($P_3{}^{15}N_3^+$) (fig. S2). The corresponding TPD profile also reveals a triplet with maxima at 216, 238, and 259 K; this finding mirrors the sublimation events at *m/z* = 135 in nonisotopically labeled experiments confirming the aforementioned assignments. In blank studies, experiments were carried out under identical conditions, but without electron processing of the ices, no ion counts at these *m/z* were detected at all (Fig. 4), demonstrating that the identified species are due to the irradiation of the ices but not from ion-molecule reactions in the gas phase. We therefore provided compelling evidence for the detection of P_3N_3 isomers **2** and/or **5**. Since their IEs are of 9.28 and 9.32 eV and are too close to each other, additional investigations are required to discriminate which isomer can be assigned to these sublimation events.

To discriminate between **2** and **5**, we conducted isomer-selective ultraviolet-visible (UV-vis) photolysis experiments (*20*, *21*). Here, the ices were first processed by energetic electrons to produce the P_3N_3 isomers and then to photolyze selectively to degrade and/or isomerize these isomers. This requires the knowledge of the UV-vis absorption spectrum of **2** and **5**. Time-dependent density functional theory (DFT) computations reveal that absorption bands at λ = 452 nm [highest occupied molecular orbital (HOMO) (E′) → lowest unoccupied molecular orbital (LUMO) (E″)] and λ = 388 nm [HOMO (A′) → LUMO +1 (A″) and HOMO −1 (A′) → LUMO +1 (A″)] are exclusive to **2** and **5**, respectively (table S4 and fig. S3). Therefore, photolysis at λ = 452 nm and λ = 388 nm for 1 hour with 30 mW selectively isomerizes and/or photolyzes isomers **2** and **5**, respectively. A comparison of the TPD graph at *m/z* = 135 of the electron irradiation system (Fig. 4A) with the photolyzed sample (452 nm; absorption band of **2**; Fig. 4C) reveals that the 256-K sublimation event vanishes; the 215- and 237-K peaks are still present. On the other hand, 388-nm photolysis (absorption of **5**) leads to the disappearance of the 237-K sublimation event, but the peaks at 215

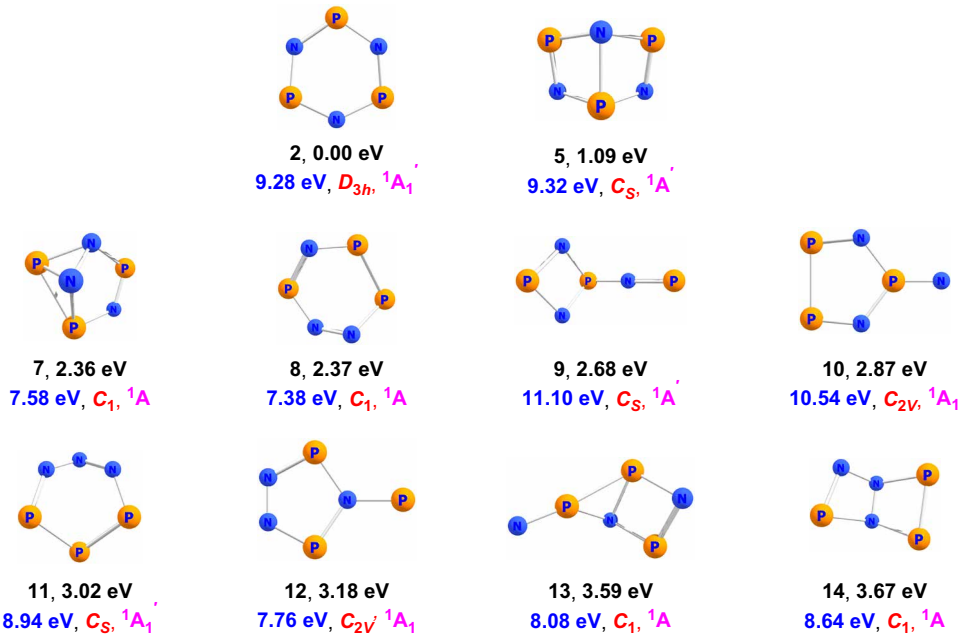

Fig. 2. Molecular structures of P_3N_3 isomers. Relative energies in electron volts (black), adiabatic IEs in electron volts (blue), point groups (red), and ground states (magenta) are also shown. The energies were computed at the CCSD(T)/CBS//B3LYP/cc-pVTZ level of theory and include zero-point vibrational energy (ZPVE) corrections.

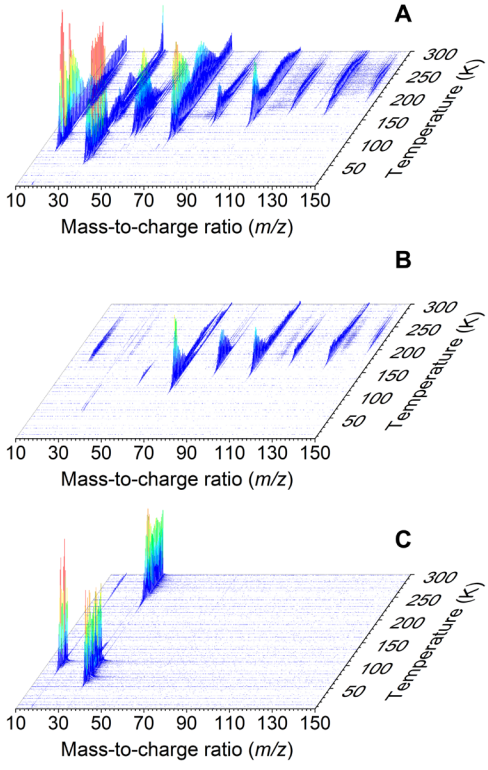

Fig. 3. PI-ReTOF-MS data during the TPD phase of the phosphine (PH_3) and ammonia (NH_3) ice mixtures. (**A**) Electron processed ice, PE = 10.49 eV. (**B**) Electron processed ice, PE = 9.10 eV. (**C**) Pristine ice, PE = 10.49 eV.

and 256 K still remain (Fig. 4D). The phenomena are not due to laser-induced thermal decomposition, as the temperature of the sample was kept at 5 K during the photolysis. It is highly unlikely that the two experiments could generate new species, which would selectively react with the carriers of the 237- and 256-K peaks. Therefore, our results demonstrate that the 237- and 256-K peaks can be linked to two distinct P_3N_3 isomers **5** and **2**, respectively. Note that the 452-nm irradiation also results in a new peak at 200 K, which can be assigned to P_3N_3 isomers holding IEs less than 10.49 eV [**7** (IE = 7.58 eV), **8** (IE = 7.38 eV), **11** (IE = 8.94 eV), **12** (IE = 7.76 eV), **13** (IE = 8.08 eV), or **14** (IE = 8.64 eV), except **5** as it sublimes at 256 K]. These new species may be generated by isomerization of **2** or reactions of other molecules within the ice induced by blue light irradiation. No new peak is observed in the TPD profile of m/z = 135 recorded in the 388-nm photolysis, suggesting that **5** either rearranges to isomers having IEs higher than 10.49 eV [**9** (IE = 11.10 eV) and **10** (IE = 10.54 eV)] or fragments to smaller molecules, e.g., PN.

Structure and aromaticity

Having established the formation of the P_3N_3 isomers **2** and **5**, we are shifting our attention now to their electronic and geometric structures. For isomer **5**, the length of both P═N bonds is 1.62 Å at the CCSD(T)/cc-pVTZ level of theory, while the remaining P—N single bonds are 0.11 to 0.25 Å longer (table S3); this is similar to the C—C bond lengths in Dewar benzene (*22*). In **2**, all six P—N bonds have a length of 1.64 Å (table S3); this bond length is shorter than P—N bonds in saturated phosphazanes (1.77 Å) (*23*), which indicates partial double bond character. Conjugation-induced shortening of the P—N bond from saturated species (−0.13 Å) is similar to that of the C—C bond of isovalent benzene (C_6H_6, **4**) (−0.14 Å). The aromatic character of **2** can be evaluated from NICS values (vide supra) and homodesmotic equations (Fig. 5). We computed the NICS(0) (h = 0.0 Å) and NICS(1) (h = 1.0 Å) values for benzene (C_6H_6, **4**), borazine ($B_3N_3H_6$, **15**), and **2** (table S5). The NICS(0) values for benzene (C_6H_6, **4**) and borazine ($B_3N_3H_6$, **15**) are negative (−8.2 and −1.7 ppm), while for **2**, a positive value ensues (+2.8 ppm). All computed NICS(1) values are negative (−10.4, −3.0, and − 3.5 ppm), indicating the deshielding and π-aromatic character (to view the π

orbitals of **2**, see fig. S4) for all compounds. NICS values for **2** become negative at h = 0.5 Å and reach a maximum at h = 1.2 Å (−3.8 ppm), which is still remarkably lower than in benzene (C_6H_6, **4**) (maximum at h = 0.8 Å, −10.7 ppm; table S5). An explanation might be the larger atomic radii of phosphorus in comparison to carbon. According to the NICS aromaticity criteria, **2** would be almost three times less aromatic than **4** and shows similar aromaticity as borazine ($B_3N_3H_6$, **15**). We computed the aromatic stabilizations of **2**, benzene (C_6H_6, **4**), and borazine ($B_3N_3H_6$, **15**). With the help of the homodesmotic equations (*24*) depicted in Fig. 5, cyclohexene (**16**) reacts in a hypothetical reaction with cyclohexadiene (**17**) to form cyclohexane (**18**) and benzene (C_6H_6, **4**). The reaction enthalpy ΔH_r^0 equals the aromatic and conjugative stabilization of benzene (C_6H_6, **4**) and is computed to be $\Delta H_r^0 = -151$ kJ mol^{-1}. The reaction enthalpies for borazine ($B_3N_3H_6$, **15**) and **2** are computed with similar equations (Fig. 5, II and III) to be $\Delta H_r^0 = -233$ kJ mol^{-1} and $\Delta H_r^0 = -45$ kJ mol^{-1}. Benzene is almost three times more stable than **2**, in line with our NICS(1) computations. However, borazine ($B_3N_3H_6$, **15**) seems to be the most stable one. These numbers might explain why benzene (C_6H_6, **4**) and borazine ($B_3N_3H_6$, **15**) are easy to synthesize and bench stable, while the formation and isolation of **2** are highly challenging.

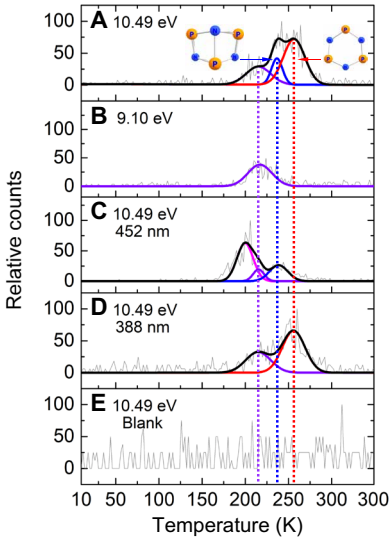

Fig. 4. PI-ReTOF-MS data at *m/z* = 135 during the TPD phase of the phosphine (PH_3) and ammonia (NH_3) ice mixtures. (**A**) Electron processed ice, PE = 10.49 eV. (**B**) Electron processed ice, PE = 9.10 eV. (**C**) Electron and 452-nm laser–processed ice, PE = 10.49 eV. (**D**) Electron and 388-nm laser–processed ice, PE = 10.49 eV. (**E**) Pristine ice, PE = 10.49 eV.

DISCUSSION

We prepared the highly reactive cyclotriphosphazene (P_3N_3, **2**) along with its Dewar benzene–type isomer 1,3,5-triphosha-2,4,6-triazabicyclo [2.2.0]hexa-2,5-diene (P_3N_3, **5**) in ammonia- phosphine ices exposed to energetic electrons and also explored their photoreactions at λ = 452 nm and λ = 388 nm. Both isomers were detected in the gas phase upon sublimation of the newly formed molecules exploiting tunable, single PI-ReTOF-MS. Considering the average velocity of 200 m s^{-1} of **2** and **5** subliming in the 230- to 300-K range and the 2-mm distance between the ice and the photoionization laser, the lifetimes of both neutral isomers in the gas phase have to be at least 8 μs to survive the flight time from sublimation and photoionization. Structure **2** is the parent to a broad variety of phosphacyclic compounds that have been extensively applied in various areas, such as biomedicine, nanotechnology, and catalysis (*12*, *13*, *25*, *26*). This work

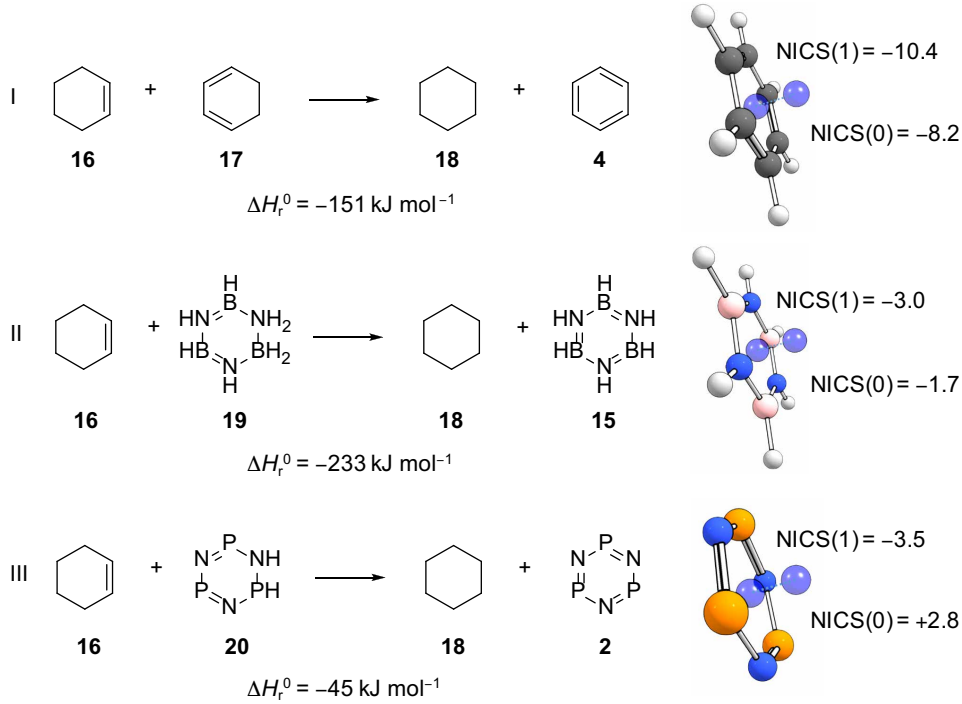

Fig. 5. Homodesmotic equations (I to III) for the determination of the aromatic stabilization of benzene (4), borazine (15), and cyclotriphosphazene (2) and computed NICS values (given in parts per million, ppm) at the B3LYP/cc-pVTZ level of theory.

represents a versatile benchmark to prepare and identify highly reactive molecules isomer selectively by coupling distinct photochemistry schemes with soft photoionization.

MATERIALS AND METHODS

Experimental

The experiments were performed at the W. M. Keck Research Laboratory in Astrochemistry (*19*). The experimental setup consists of a contamination-free stainless steel ultrahigh vacuum chamber (UHV) evacuated to a base pressure of a few 10^{-11} torr by magnetically levitated turbo molecular pumps coupled to oil-free scroll backing pumps. Within the chamber, a silver mirror substrate is interfaced to a cold finger, which is connected to a closed cycle helium compressor (Sumitomo Heavy Industries, RDK-415E). Using a doubly differentially pumped rotational feedthrough (Thermionics Vacuum Products, RNN-600/FA/ MCO) and an UHV compatible bellow (McAllister, BLT106), the substrate is able to be rotated in the horizontal plane and to be translated vertically, respectively. The temperature of the silver wafer was monitored by a silicon diode sensor (Lakeshore DT-470) and regulated in a range of 5 to 300 K with a precision of ±0.1 K by a programmable temperature controller (Lakeshore 336). After the wafer reached 5.0 ± 0.1 K, phosphine (PH_3; Sigma-Aldrich; 99.9995%) and ammonia (NH_3; Matheson; 99.9992%) (table S1) were codeposited onto it via two glass capillary arrays to form an ice with a PH_3:NH_3 = (1.5 ± 0.3):1 composition ratio. Isotopically labeled ^{15}N-ammonia ($^{15}NH_3$; Sigma-Aldrich; 98% ^{15}N) were used in duplicate experiments to observe infrared absorption and mass shifts of products. We also performed experiments using D_3-ammonia (ND_3) but detected a strong signal from D_5-tetraphosphane (P_4D_5H) (*m/z* = 135) (*14*), which obscured the signal from our target P_3N_3 molecules (*m/z* = 135). The overall thickness of the ice was determined using laser interferometry (*27*), with one helium-neon laser (CVI Melles Griot, 25-LHP-230) operating at 632.8 nm. The laser light was reflected at an angle of 2° relative to the ice surface normal. Considering that the ratio of PH_3 and NH_3 = (1.5 ± 0.3):1 and that the refractive indices of pure ices n_{PH3} = 1.51 ± 0.04 and n_{NH3} = 1.41 ± 0.04 (*14*, *28*), the ice thickness was calculated to be 1400 ± 70 nm.

Mid-infrared (6000 to 400 cm^{-1}) spectra of the ices were recorded using a Nicolet 6700 FTIR spectrometer with 4-cm^{-1} spectral resolution. The FTIR spectra of the pristine ice are shown in fig. S1. Detailed assignments of the peaks are compiled in table S2 (*14*–*18*, *28*). The ice composition was determined via a modified Beer-Lambert law (*14*). The average column density of PH_3 was calculated to be (1.9 ± 0.3) × 10^{18} molecules cm^{-2} based on the integrated areas along with absorption coefficients of 4.7 × 10^{-18} and 5.1 × 10^{-19} cm $molecule^{-1}$ for the 2319-cm^{-1} (ν_1/ν_1) and 983-cm^{-1} (ν_2) bands (*14*), respectively. For NH_3, the average column density was determined to be (1.2 ± 0.2) × 10^{18} molecules cm^{-2} based on the integrated areas along with absorption coefficients of 2.1 × 10^{-17}, 5.0 × 10^{-18}, and 2.1 × 10^{-17} cm $molecule^{-1}$ for the 3366-cm^{-1} (ν_4), 1625-cm^{-1} (ν_4), and 1053-cm^{-1} (ν_2) bands (*28*), respectively. Therefore, the ratio of PH_3 and NH_3 is (1.5 ± 0.3):1. Taking into account the densities of PH_3 (0.9 g cm^{-1}) (*14*) and NH_3 (0.74 ± 0.02 g cm^{-1}) (*28*), the total ice thickness was found to be 1650 ± 300 nm, which is consistent with the value obtained from the laser interferometry method (1400 ± 70 nm).

The ices were then isothermally irradiated at 5.0 ± 0.1 K with 5-keV electrons (Specs EQ 22/35 electron source) at a 70° angle to the ice surface normal for 2 hours at currents of 0 nA (blank) and 100 nA (table S1). Using Monte Carlo simulations (CASINO 2.42) (*29*), the average and maximum penetration depths of the electrons were calculated to be 360 ± 40 nm and 830 ± 90 nm, respectively (table S1), which are less than the 1400 ± 70–nm ice thickness, ensuring no interaction between the impinging electrons and the silver substrate. With the parameters compiled in table S1, the irradiation doses at 100 nA were calculated to be 30.99 ± 5.10 eV per PH_3 molecule and 15.49 ± 2.54 eV per NH_3 molecule. During the irradiation, in situ mid-infrared spectra of the ices were recorded every 2 min.

After the irradiation, the ices were directly warmed to 300 K at a rate of 1 K min^{-1} (TPD) or first irradiated by 452- or 388-nm laser light at 30 mW for 1 hour and then annealed to 300 K at 1 K min^{-1}. The 452- and 388-nm laser lights were generated using the third harmonic (355 nm) of a pulsed neodymium-doped yttrium aluminum garnet (Nd:YAG) laser (30 Hz; Spectra Physics, PRO-270) to pump a coumarin 450 dye [ethanol (0.20 g $liter^{-1}$)] and an LD 390 dye [ethanol (0.37 g $liter^{-1}$)], respectively. During the TPD phase, any subliming molecules were detected using a ReTOF-MS (Jordon TOF Products Inc.) with single-photon ionization (*19*) (Figs. 3 and 4 and fig. S2). This photoionization process uses difference four-wave mixing to produce vacuum UV (VUV) light ($\omega_{vuv} = 2\omega_1 - \omega_2$) (table S1). The experiments were performed with 10.49-eV photoionization energy and repeated at 9.10 eV to distinguish between the P_3N_3 isomers. The 10.49-eV (118.222 nm) light was generated via frequency tripling ($\omega_{vuv} = 3\omega_1$) of the third harmonic (355 nm) of the fundamental of a Nd:YAG laser (YAG A) in pulsed gas jets of Xe. To produce 9.10 eV, the third harmonic (355 nm) of a Nd:YAG laser was used to pump a coumarin 450 dye [ethanol (0.20 g $liter^{-1}$)] to obtain 445.132 nm (2.72 eV; Sirah, Cobra-Stretch), which underwent a frequency doubling process to achieve ω_1 = 222.566 nm (5.57 eV) (β-BaB_2O_4 crystals, 57.4°). A second Nd:YAG laser (second harmonic at 532 nm) pumped rhodamine 610/640 dye mixture [ethanol (0.17/0.04 g $liter^{-1}$)] to obtain ω_2 = 607 nm (2.04 eV), which then combined with $2\omega_1$, using xenon as a nonlinear medium and generated ω_{vuv} = 136.246 nm (9.10 eV) at 10^{12} photons per pulse. The VUV light was spatially separated from other wavelengths [due to multiple resonant and nonresonant processes ($2\omega_1 + \omega_2$; $3\omega_1$; $3\omega_2$)] using a lithium fluoride biconvex lens (ISP Optics) and directed 2 mm above the sample to ionize subliming molecules. The ionized molecules were mass analyzed with the ReTOF-MS, where the arrival time to a multichannel plate is based on *m/z*, and the signal was amplified with a fast preamplifier (Ortec 9305) and recorded with a personal computer multichannel scalar (FAST ComTec, P7888-1E), which is triggered via a pulse delay generator at 30 Hz. Here, the ReTOF signal is the average of 3600 sweeps of the mass spectrum in 4-ns bin widths, which corresponds to an increase in the substrate temperature of 2 K.

Theoretical

All computations were carried out with Gaussian 16 Revision A.03 (*30*) (Figs. 2 and 5, figs. S3 and S4, and tables S3 to S5). For geometry optimizations and frequency computations, the DFT B3LYP functional (*31*–*33*) was used with the Dunning correlation-consistent split valence basis set cc-pVTZ (*34*). On the basis of these geometries, the corresponding frozen core–coupled cluster (*35*–*38*) CCSD(T)/cc-pVDZ, CCSD(T)/cc-pVTZ, and CCSD(T)/cc-pVQZ single-point energies were computed and extrapolated to complete basis set limit (*39*) CCSD(T)/CBS with B3LYP/cc-pVTZ zero-point vibrational energy (ZPVE) corrections. The adiabatic IEs were computed by

taking the ZPVE-corrected energy difference between the neutral and ionic species that correspond to similar conformations. The UV-vis spectra for cyclotriphosphazene (P_3N_3 isomer, **2**) and 1,3,5-triphosha-2,4,6-triazabicyclo[2.2.0]hexa-2,5-diene (P_3N_3 isomer, **5**) were computed using TD-B3LYP method with a cc-pVTZ basis set. For all TD-B3LYP computations, 16 transitions into the first excited singlet state were computed. The geometries and frequencies of **2** and **5** were also computed at the CCSD(T)/cc-pVTZ level of theory. NICSs were computed at the B3LYP/cc-pVTZ level of theory. Natural bond orbitals were computed with the NBO6 program (*40*).

SUPPLEMENTARY MATERIALS

Supplementary material for this article is available at http://advances.sciencemag.org/cgi/content/full/6/30/eaba6934/DC1

REFERENCES AND NOTES

1. R. L. Melen, Frontiers in molecular p-block chemistry: From structure to reactivity. *Science* **363**, 479–484 (2019).
2. A. Velian, C. C. Cummins, Synthesis and characterization of $P_2N_3^-$: An aromatic ion composed of phosphorus and nitrogen. *Science* **348**, 1001–1004 (2015).
3. R. M. Atkins, P. L. Timms, The matrix infrared spectrum of PN and SiS. *Spectrochim. Acta A Mol. Spectrosc.* **33**, 853–857 (1977).
4. R. Ahlrichs, M. Bär, H. S. Plitt, H. Schnöckel, The stability of PN and $(PN)_3$. Ab initio calculations and matrix infrared investigations. *Chem. Phys. Lett.* **161**, 179–184 (1989).
5. J. O. Jensen, Vibrational frequencies and structural determination of cyclotriphosphazene. *J. Mol. Struct. Theochem.* **729**, 229–234 (2005).
6. G. Sánchez-Sanz, Aromatic behaviour of benzene and naphthalene upon pnictogen substitution. *Tetrahedron* **71**, 826–839 (2015).
7. E. Elguero, I. Alkorta, J. Elguero, A theoretical study of the properties of ninety-two "aromatic" six-membered rings including benzene, azines, phosphinines and azaphosphinines. *Heteroatom Chem.* **29**, e21441 (2018).
8. A. A. Starikova, N. M. Boldyreva, R. M. Minyaev, A. I. Boldyrev, V. I. Minkin, Computational assessment of an elusive aromatic N_3P_3 molecule. *ACS Omega* **3**, 286–291 (2018).
9. E. Hückel, Quantentheoretische Beiträge zum Benzolproblem. *Z. Phys. A Hadron. Nucl.* **70**, 204–286 (1931).
10. P. B. Karadakov, Ground-and excited-state aromaticity and antiaromaticity in benzene and cyclobutadiene. *J. Phys. Chem. A* **112**, 7303–7309 (2008).
11. H. Tokoyama, H. Yamakado, S. Maeda, K. Ohno, Isomers of benzene on its global network of reaction pathways. *B. Chem. Soc. Jpn.* **88**, 1284–1290 (2015).
12. L. Wang, Y.-X. Yang, X. Shi, S. Mignani, A.-M. Caminade, J.-P. Majoral, Cyclotriphosphazene core-based dendrimers for biomedical applications: An update on recent advances. *J. Mater. Chem. B* **6**, 884–895 (2018).
13. A. Tataroğlu, F. Özen, K. Koran, A. Dere, A. O. Görgülü, N. Al-Senany, A. Al-Ghamdi, W. A. Farooq, F. Yakuphanoglu, Structural, electrical and photoresponse properties of Si-based diode with organic interfacial layer containing novel cyclotriphosphazene compound. *Silicon* **10**, 683–691 (2018).
14. A. M. Turner, M. J. Abplanalp, S. Y. Chen, Y. T. Chen, A. H. H. Chang, R. I. Kaiser, A photoionization mass spectroscopic study on the formation of phosphanes in low temperature phosphine ices. *Phys. Chem. Chem. Phys.* **17**, 27281–27291 (2015).
15. T. Shimanouchi, Tables of molecular vibrational frequencies. Consolidated volume II. *J. Phys. Chem. Ref. Data* **6**, 993–1102 (1977).
16. G. Socrates, *Infrared and Raman Characteristic Group Frequencies* (John Wiley & Sons Ltd., ed. 3, 2004).
17. J. H. Teles, G. Maier, B. Andes Hess Jr., L. J. Schaad, Infrared spectra and photochemistry of isodiazene and its deuterated isotopomers. *Chem. Ber.* **122**, 749–752 (1989).
18. W. Zheng, D. Jewitt, Y. Osamura, R. I. Kaiser, Formation of nitrogen and hydrogen-bearing molecules in solid ammonia and implications for solar system and interstellar ices. *Astrophys. J.* **674**, 1242–1250 (2008).
19. B. M. Jones, R. I. Kaiser, Application of reflectron time-of-flight mass spectroscopy in the analysis of astrophysically relevant ices exposed to ionization radiation: Methane (CH_4) and D4-methane (CD_4) as a case study. *J. Phys. Chem. Lett.* **4**, 1965–1971 (2013).
20. M. Irie, T. Fukaminato, T. Sasaki, N. Tamai, T. Kawai, Organic chemistry: A digital fluorescent molecular photoswitch. *Nature* **420**, 759–760 (2002).
21. S. Kobatake, S. Takami, H. Muto, T. Ishikawa, M. Irie, Rapid and reversible shape changes of molecular crystals on photoirradiation. *Nature* **446**, 778–781 (2007).
22. J. O. Jensen, Vibrational frequencies and structural determination of Dewar benzene. *J. Mol. Struc. Theochem* **680**, 227–236 (2004).
23. A. B. Chaplin, J. A. Harrison, P. J. Dyson, Revisiting the electronic structure of phosphazenes. *Inorg. Chem.* **44**, 8407–8417 (2005).
24. S. E. Wheeler, K. N. Houk, P. v. R. Schleyer, W. D. Allen, A hierarchy of homodesmotic reactions for thermochemistry. *J. Am. Chem. Soc.* **131**, 2547–2560 (2009).
25. J. Barberá, M. Bardají, J. Jiménez, A. Laguna, M. P. Martínez, L. Oriol, J. L. Serrano, I. Zaragozano, Columnar mesomorphic organizations in cyclotriphosphazenes. *J. Am. Chem. Soc.* **127**, 8994–9002 (2005).
26. E. Blattes, A. Vercellone, H. Eutamène, C.-O. Turrin, V. Théodorou, J.-P. Majoral, A.-M. Caminade, J. Prandi, J. Nigou, G. Puzo, Mannodendrimers prevent acute lung inflammation by inhibiting neutrophil recruitment. *Proc. Natl. Acad. Sci. U.S.A.* **110**, 8795–8800 (2013).
27. L. Zhou, S. Maity, M. Abplanalp, A. Turner, R. I. Kaiser, On the radiolysis of ethylene ices by energetic electrons and implications to the extraterrestrial hydrocarbon chemistry. *Astrophys. J.* **790**, 38 (2014).
28. M. Bouilloud, N. Fray, Y. Bénilan, H. Cottin, M.-C. Gazeau, A. Jolly, Bibliographic review and new measurements of the infrared band strengths of pure molecules at 25 K: H_2O, CO_2, CO, CH_4, NH_3, CH_3OH, HCOOH and H_2CO. *Mon. Not. Roy. Astron. Soc.* **451**, 2145–2160 (2015).
29. D. Drouin, A. R. Couture, D. Joly, X. Tastet, V. Aimez, R. Gauvin, CASINO V2.42—A fast and easy-to-use modeling tool for scanning electron microscopy and microanalysis users. *Scanning* **29**, 92–101 (2007).
30. M. J. Frisch, G. W. Trucks, H. B. Schlegel, G. E. Scuseria, M. A. Robb, J. R. Cheeseman, G. Scalmani, V. Barone, G. A. Petersson, H. Nakatsuji, X. Li, M. Caricato, A. V. Marenich, J. Bloino, B. G. Janesko, R. Gomperts, B. Mennucci, H. P. Hratchian, J. V. Ortiz, A. F. Izmaylov, J. L. Sonnenberg, D. Williams-Young, F. Ding, F. Lipparini, F. Egidi, J. Goings, B. Peng, A. Petrone, T. Henderson, D. Ranasinghe, V. G. Zakrzewski, J. Gao, N. Rega, G. Zheng, W. Liang, M. Hada, M. Ehara, K. Toyota, R. Fukuda, J. Hasegawa, M. Ishida, T. Nakajima, Y. Honda, O. Kitao, H. Nakai, T. Vreven, K. Throssell, J. A. Montgomery Jr., J. E. Peralta, F. Ogliaro, M. J. Bearpark, J. J. Heyd, E. N. Brothers, K. N. Kudin, V. N. Staroverov, T. A. Keith, R. Kobayashi, J. Normand, K. Raghavachari, A. P. Rendell, J. C. Burant, S. S. Iyengar, J. Tomasi, M. Cossi, J. M. Millam, M. Klene, C. Adamo, R. Cammi, J. W. Ochterski, R. L. Martin, K. Morokuma, O. Farkas, J. B. Foresman, D. J. Fox, *Gaussian 16, Revision A.03* (Gaussian Inc., 2016).
31. A. D. Becke, Density-functional exchange-energy approximation with correct asymptotic behavior. *Phys. Rev. A* **38**, 3098–3100 (1988).
32. A. D. Becke, Density-functional thermochemistry. III. The role of exact exchange. *J. Chem. Phys.* **98**, 5648–5652 (1993).
33. C. Lee, W. Yang, R. G. Parr, Development of the Colle-Salvetti correlation-energy formula into a functional of the electron density. *Phys. Rev. B* **37**, 785–789 (1988).
34. T. H. Dunning Jr., Gaussian basis sets for use in correlated molecular calculations. I. The atoms boron through neon and hydrogen. *J. Chem. Phys.* **90**, 1007–1023 (1989).
35. J. Čížek, On the correlation problem in atomic and molecular systems. Calculation of wavefunction components in Ursell-type expansion using quantum-field theoretical methods. *J. Chem. Phys.* **45**, 4256–4266 (1966).
36. R. J. Bartlett, J. D. Watts, S. A. Kucharski, J. Noga, Non-iterative fifth-order triple and quadruple excitation energy corrections in correlated methods. *Chem. Phys. Lett.* **165**, 513–522 (1990).
37. K. Raghavachari, Electron correlation techniques in quantum chemistry: Recent advances. *Annu. Rev. Phys. Chem.* **42**, 615–642 (1991).
38. J. F. Stanton, Why CCSD(T) works: A different perspective. *Chem. Phys. Lett.* **281**, 130–134 (1997).
39. K. A. Peterson, D. E. Woon, T. H. Dunning Jr., Benchmark calculations with correlated molecular wave functions. IV. The classical barrier height of the H $+H_2 \rightarrow H_2 + H$ reaction. *J. Chem. Phys.* **100**, 7410–7415 (1994).
40. E. D. Glendening, J. K. Badenhoop, A. E. Reed, J. E. Carpenter, J. A. Bohmann, C. M. Morales, C. R. Landis, F. Weinhold, *NBO, Version 6.0* (Theoretical Chemistry Institute, University of Wisconsin, 2013).

Acknowledgments: We thank J. LaJeunesse for helping perform the experiments. **Funding:** This work was supported by NASA under grant NNX16AD27G to the University of Hawaii (to R.I.K.). The data analysis and preparation of the manuscript were partially financed by the Alexander von Humboldt Foundation (Feodor Lynen Research Fellowship to A.K.E.). **Author contributions:** R.I.K. designed the experiments. C.Z., A.K.E., A.B., and S.K.S. performed the experiments. A.K.E. and P.R.S. carried out the theoretical analysis and designed the UV-vis photolysis experiments. C.Z., A.K.E., and R.I.K. wrote the manuscript, which was read, revised, and approved by all co-authors. **Competing interests:** The authors declare that they have no competing interests. **Data and materials availability:** All data needed to evaluate the conclusions in the paper are present in the paper and/or the Supplementary Materials. Additional data related to this paper may be requested from the authors.

Submitted 24 December 2019
Accepted 8 June 2020
Published 22 July 2020
10.1126/sciadv.aba6934

Citation: C. Zhu, A. K. Eckhardt, A. Bergantini, S. K. Singh, P. R. Schreiner, R. I. Kaiser, The elusive cyclotriphosphazene molecule and its Dewar benzene–type valence isomer (P_3N_3). *Sci. Adv.* **6**, eaba6934 (2020).